

# 3D Face Modeling via Weakly-supervised Disentanglement Network joint Identity-consistency Prior

Guohao Li<sup>1</sup>, Hongyu Yang<sup>2,3</sup>, Di Huang<sup>1</sup> and Yunhong Wang<sup>1</sup>

<sup>1</sup> School of Computer Science and Engineering, Beihang University, Beijing, China

<sup>2</sup> Institute of Artificial Intelligence, Beihang University, Beijing, China

<sup>3</sup> Shanghai Artificial Intelligence Laboratory, Shanghai, China

{liguohao, hongyuyang, dhuang, yhwang}@buaa.edu.cn

**Abstract**—Generative 3D face models featuring disentangled controlling factors hold immense potential for diverse applications in computer vision and computer graphics. However, previous 3D face modeling methods face a challenge as they demand specific labels to effectively disentangle these factors. This becomes particularly problematic when integrating multiple 3D face datasets to improve the generalization of the model. Addressing this issue, this paper introduces a Weakly-Supervised Disentanglement Framework, denoted as WSDF, to facilitate the training of controllable 3D face models without an overly stringent labeling requirement. Adhering to the paradigm of Variational Autoencoders (VAEs), the proposed model achieves disentanglement of identity and expression controlling factors through a two-branch encoder equipped with dedicated identity-consistency prior. It then faithfully re-entangles these factors via a tensor-based combination mechanism. Notably, the introduction of the Neutral Bank allows precise acquisition of subject-specific information using only identity labels, thereby averting degeneration due to insufficient supervision. Additionally, the framework incorporates a label-free second-order loss function for the expression factor to regulate deformation space and eliminate extraneous information, resulting in enhanced disentanglement. Extensive experiments have been conducted to substantiate the superior performance of WSDF. Our code is available at [github.com/liguohao96/WSDF](https://github.com/liguohao96/WSDF).

## I. INTRODUCTION

3D face modeling is a persistent topic due to its numerous applications in discriminative and generative tasks within 2D and 3D domains, such as 2D face recognition [30], [56], facial attribute transfer [46], 3D face reconstruction [14] and virtual avatars [21], [44]. The versatility of 3D face modeling stems from its controllable and generative capabilities, enabling the representation and generation of 3D faces with disentangled, interpretable, and editable factors.

Linear 3D Morphable Models (3DMMs) [4], [5], [1], [17] achieve controllable generation of facial geometry by separately modeling identity and expression deformation through Principal Component Analysis (PCA) applied to 3D facial scans annotated with both identity and expression labels. To enhance performance, dense expression labels are utilized in constructing multi-linear models [51], [52], [8]. Unfortunately, the limited representation ability of linear models and the scarcity of expression-annotated 3D facial scans hinder the generalizability of these methods. The advent of deep learning has spurred the exploration of non-linear models, employing explicit [2], [39], [7], [29], [13]

or implicit modeling [57], [62], [60], leveraging training data from both 2D images [48], [47], [49] and 3D scans [29], [3] for improved generalizability. Nevertheless, the persistent need for expression labels [45], [38], [29], [62], [44] to achieve identity and expression disentanglement remains an unresolved challenge. Since 3D face datasets are often collected and labeled for diverse purposes, and joint expression labels are typically unavailable, existing methods are confined to a limited number of 3D facial datasets with dedicated expression labels. This limitation becomes a significant obstacle when attempting to combine multiple datasets to enhance diversity, ultimately compromising the overall generalizability.

Recent studies have demonstrated the remarkable capability of generative models in disentangling latent spaces [20], [10], [25], [54], [44]. Furthermore, insights from [31] underscore the importance of introducing inductive biases on data or models for effective representation disentanglement. Notably, these studies propose an alternative training scheme for 3DMMs, suggesting that the need for explicit expression labels can be circumvented. This is achieved by treating facial expression as a complementary, identity-irrelevant factor, leveraging the abundance of identity information in almost all existing 3D face datasets. To our knowledge, Gu *et al.* are pioneers in exploring such inductive bias to separate identity and expression latent spaces [19]. However, it is worth noting that their use of adversarial training to implicitly learn identity information is not foolproof in preventing local minima arising from the ambiguity of weak supervision. Both whole and partial identity-relevant information may satisfy identity-consistency, as highlighted in [41], [19].

This paper focuses on advancing 3D facial shape modeling and introduces an innovative 3D Morphable Model (3DMM) that effectively disentangles identity and expression representations using only weak supervision provided by identity labels. Our approach utilizes a topology-consistent mesh to represent 3D geometries, chosen for its efficiency in generation, editing, and rendering tasks. The model adopts a VAE-based paradigm, employing two encoders to learn identity and expression latent spaces and re-coupling them during decoding to generate 3D faces. A key feature of our model is its handling of the ambiguity in identity representations when relying solely on identity-consistency. To address this, we introduce dedicated constraints to achieve

disentanglement and impose an identity-consistency prior. Specifically, we introduce the Neutral Bank module, which obtains pseudo-neutral scans for each subject by aggregating multiple samples. This module enhances the consistency of the identity branch by retaining identity-related information through the maximization of mutual information. For the expression branch, we employ a second-order loss with regularized morphing energy to induce encoding variations of expression in diverse directions within the latent space. This strategy effectively removes extraneous information from the expression space. Additionally, we propose a non-linear tensor-based fusion mechanism to combine these disentangled latent spaces, accurately modeling subject-specified expressions.

In summary, this study makes several key contributions:

- **Neutral Bank Module:** We introduce a Neutral Bank module, complemented by a dedicated loss function. This module plays a crucial role in preventing the degeneration of identity-consistency, thereby facilitating the disentanglement of the identity factor.
- **Label-Free Second-Order Loss:** We propose a label-free second-order loss, designed to enhance disentanglement by eliminating nuisance information within the expression space. This is achieved through the regularization of deformation, resulting in more effective disentanglement.
- **A novel 3DMM:** We present a novel 3DMM, namely WSDF, which is learned from combined datasets. Experimental validation demonstrates its significantly improved generalizability, marking it as an advancement in the field of 3D facial shape modeling.

## II. RELATED WORK

**3D Face Modeling.** [4], [5] propose generative 3DMM that models 3D human faces with disentangled factors facilitating controllability. The vanilla 3DMM separately models geometry and appearance of human face with two sets of linear bases. Subsequent 3DMMs [1], [35], [17], [27], [42] are proposed to improve the controllability of generative modeling by disentangling more diverse factors with dedicated supervisions. While controllability is essential, another line of interest is generalizability, which involves both realistic reconstruction and diverse generation. To improve this ability, a large amount of training data are typically required. A large scale face model (LSFM) [6] is build from non-public scans of 9,663 subjects within neutral expression. The most commonly used FLAME model, build by [27], uses a total 33,000 3D scans from 4D videos with the aid of 3D-artist. Different from the studies above, [36] circumvent the scarcity of 3D facial scans by combining multiple 3D face models. However, the generalizability is restricted by model linearity and inability to automatically learn from large-scale unlabeled scans.

More recently, the development of neural networks has facilitated the creation of nonlinear models for 3D facial geometry. By adopting differentiable rendering, 3DMMs can be learned from in-the-wild 2D images [48], [47], [49]

through solving inverse render problems during training. The models can also be trained in an end-to-end manner on 3D scans using an encoder-decoder framework [2], [29], [3], [13]. Furthermore, several methods based on Implicit Neutral Representations (INR) have been proposed [57], [62], [16], [60]. Despite achieving realistic reconstruction with powerful representations, these methods still require expression labels to disentangle geometry into identity and expression for controllability.

**3D Face Disentanglement.** Recent studies on 3D face disentanglement focused on semantically disentangling 3D face into identity and expression factors. Several approaches [28], [33] relying on dense annotations for decoupled factors have been proposed. Since labels are dataset-specified, however, these methods are not applicable to datasets with only sparse expression labels. Approaches [29], [61], [3], [53], [23], [62], [43] relax the demand for expression annotations and use only *neutral* labels as an inductive bias. They assumes that variations of neutral scans solely attribute to identity-relevant factors. However, the existence of neutral scans is still correlated with datasets, and some datasets lack such *neutral* label, *e.g.* CoMA[39]. [19] employ a discriminator to learn the inductive bias from identity-consistency and bypass the need for neutral scans, which is similar to our assumption. However, their method suffers from degenerated solutions, as shown in their experiments. Moreover, the fact that expressions are identity-specified is neglected in their additive combination of identity and expression. We prevent degeneration with information-preserving mechanism and adopt tensor-based combination to model subtle differences of the same expression category perform by different individuals.

## III. METHOD

This paper presents WSDF, a Weakly-supervised Disentanglement Network designed to learn a generative 3D face model controlled by identity and expression factors independently. The approach is based on the inductive bias of identity-consistency, which relaxes the requirements for expression annotations. In the proposed framework, to eliminate the inductive bias of model design, a two-branch encoder with an identical architecture is designed to learn disentangled latent spaces. The combination of identity and expression is achieved through a non-linear tensor-based mechanism, providing an accurate representation of subject-specified expressions. To disentangle identity, the introduction of a Neutral Bank module is pivotal, generating pseudo-neutral scans using identity labels. This module serves as supervision to enforce identity-consistency and information preservation simultaneously. To eliminate nuisance information in the expression space, a second-order loss is proposed. This loss encourages the encoding of expression variations in diverse directions and regulates the energy of these variations, contributing to improved disentanglement. Overall, WSDF presents an innovative approach to weakly-supervised disentanglement in 3D face modeling. In the

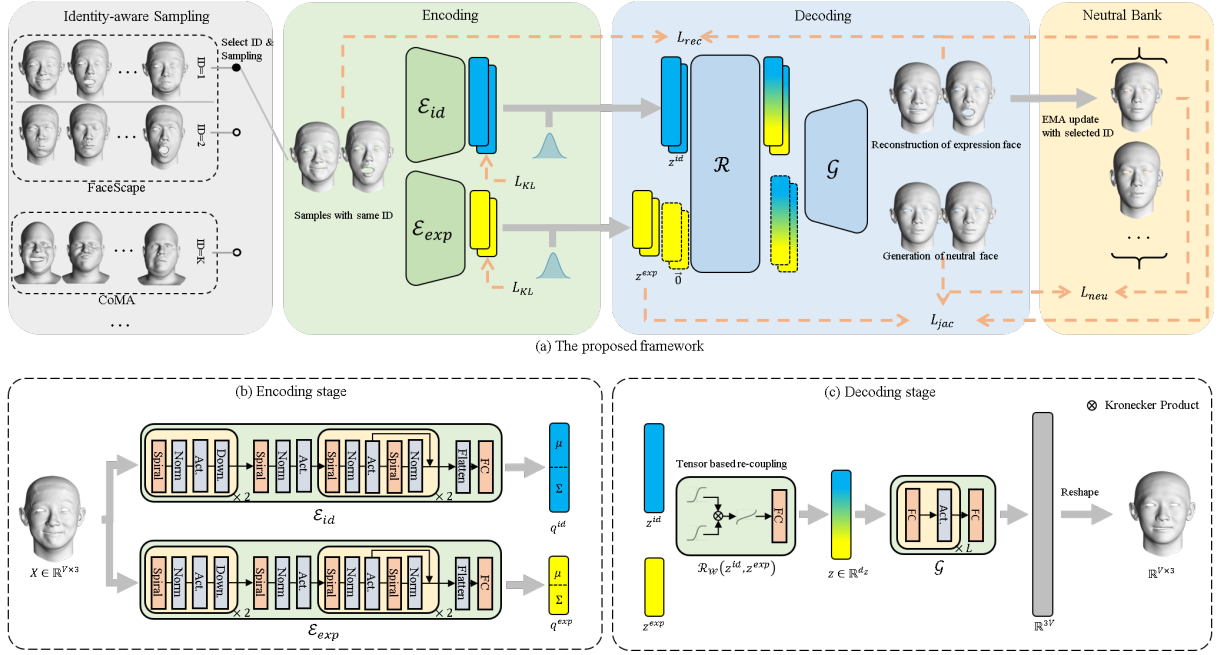


Fig. 1: Method overview. (a) Identity-aware sampling constructs a group of training samples belonging to the same ID. Two encoders,  $\mathcal{E}_{id}$  and  $\mathcal{E}_{exp}$  are built to disentangle identity and expression representations. The disentangled latent codes,  $z^{id}$  and  $z^{exp}$ , are re-coupled by fusion module  $\mathcal{R}$  and fed into the generator  $\mathcal{G}$  for decoding. Simultaneously, a neutral bank is constructed to obtain pseudo-neutral scans for each subject, imposing disentanglement through the  $\mathcal{L}_{neu}$  loss. (b) The encoders  $\mathcal{E}_{id}$  and  $\mathcal{E}_{exp}$  utilize the Spiral++ architecture with the same setup, aiming to factor out the inductive bias of model design. (c) The decoder involves a tensor-based Recoupler  $\mathcal{R}$  with non-linearity and an MLP-based  $\mathcal{G}$  for mapping from decoupled latent codes  $z^{id}$  and  $z^{exp}$  to 3D faces.

following sections, we provide a detailed description of our proposed framework and loss functions.

### A. Framework

As shown in Fig. 1(a), the proposed framework is built upon mesh-based VAEs. Two encoders,  $\mathcal{E}_{id}$  and  $\mathcal{E}_{exp}$ , are adopted to learn the decoupled latent spaces. The latent spaces are then re-coupled by tensor-based Re-coupler  $\mathcal{R}$  and fed into a generative network  $\mathcal{G}$  for reconstruction and generation. In particular, a group of 3D scans  $\{X_i\}$  belonging to the same subject is sampled from scans gathered according to IDs before training. This encoding stage could be formulated as:  $q_i^{id} = \mathcal{E}_{id}(X_i)$ ,  $q_i^{exp} = \mathcal{E}_{exp}(X_i)$ , where  $q^{id}$  and  $q^{exp}$  denote the distributions produced by  $\mathcal{E}_{id}$  and  $\mathcal{E}_{exp}$ , respectively. In the context of VAE, re-parameterization technique is utilized to draw identity latent code  $z^{id}$  and expression latent code  $z^{exp}$  for each scan from its corresponding  $q^{id}$  and  $q^{exp}$ , respectively. As shown in Fig. 1(b),  $\mathcal{E}_{id}$  and  $\mathcal{E}_{exp}$  leverage Spiral++ architecture [18] with Instance Normalization [50] and ELU activation [11].

We design a two-stage decoding pipeline, as shown in Fig. 1(c). In the first stage, the latent codes are combined together by tensor-based multiplications with non-linear functions through Re-coupler  $\mathcal{R}$ . In the second stage, a generator network  $\mathcal{G}$  is adopted to recover variations of 3D faces. This decoding stage could be formulated as:

$$X_i^r = \mathcal{G} \circ \mathcal{R}(z_i^{id}, z_i^{exp}), X_i^n = \mathcal{G} \circ \mathcal{R}(z_i^{id}, \vec{0}), \quad (1)$$

where  $X_i^r$  and  $X_i^n$  denote the reconstruction and neutralization results of input scan  $X_i$ , respectively. To maintain compatibility with previous 3DMMs, a zero vector  $\vec{0}$  is utilized to generated neutralized expression (de-expression) faces.

**Re-coupling of Factors.** To efficiently represent subject-specified expressions, we leverage a tensor-based bilinear fusion with dedicated nonlinear functions to ensure the re-coupled latent code  $z$  follows normal distribution. Without loss of generality, the tensor-based bilinear fusion could be described as  $\mathcal{W} \times_2 U^{(2)} \times_3 U^{(3)}$  where  $\mathcal{W} \in \mathbb{R}^{k \times i \times j}$  is the weight tensor,  $U^{(2)} \in \mathbb{R}^{r \times i}$  and  $U^{(3)} \in \mathbb{R}^{s \times j}$  are parameter matrices and  $\times_n$  denotes the mode- $n$  product. Despite its higher-dimensional representation, this bilinear model is equivalent to matrix multiplication as shown below:

$$\begin{aligned} (\mathcal{W} \times_2 U^{(2)} \times_3 U^{(3)})_{krs} &= \sum_{j=1}^J (\mathcal{W} \times_2 U^{(2)})_{krj} U_{sj}^{(3)} \\ &= \sum_{j=1}^J \sum_{i=1}^I \mathcal{W}_{kij} U_{ri}^{(2)} U_{sj}^{(3)} \\ &= \mathbb{M}_{\mathcal{W}}(U^{(2)} \otimes U^{(3)})^T, \end{aligned}$$

where  $\mathbb{M}_{\mathcal{W}} \in \mathbb{R}^{k \times ij}$  denotes the reshaped matrix of tensor  $\mathcal{W}$ . When it comes to our Re-coupler,  $U^{(2)}$  and  $U^{(3)}$  are replaced by the disentangled vectors  $z_i^{id}$  and  $z_i^{exp}$ , respectively. Since elements in  $z^{id}$  and  $z^{exp}$  follow a normal

distribution  $\mathcal{N}(0, 1)$ , and the product of two gaussian random variables follows a complicated distribution, the multiplied result will not preserve normal distributions. To address this issue, we adopt inverse transform sampling technique:  $z^{id}$  and  $z^{exp}$  are transformed into  $\mathbb{U}_{z^{id}}, \mathbb{U}_{z^{exp}} \sim \mathcal{U}(0, 1)$  first by non-linear function  $\mathbb{U}$ , then the multiplied result  $\mathbb{U}_{z^{id}} \otimes \mathbb{U}_{z^{exp}}$  is transformed into  $\mathbb{N}_{\mathbb{U}_{z^{id}} \otimes \mathbb{U}_{z^{exp}}} \sim \mathcal{N}(0, 1)$  by non-linear function  $\mathbb{N}$ . Finally, these normal distribution variables are linear combined by  $\mathbb{M}_{\mathcal{W}}$ . Although the elements of  $\mathbb{N}_{\mathbb{U}_{z^{id}} \otimes \mathbb{U}_{z^{exp}}}$  are dependent, we treat them as independent ones and use a normalized  $\mathbb{M}_{\mathcal{W}}$  to ensure the variance of  $z$  is 1. Formally, the proposed Re-coupler is defined as:

$$\mathcal{R}_{\mathcal{W}}(z^{id}, z^{exp}) = \mathbb{M}_{\mathcal{W}} \mathbb{N}_{\mathbb{U}_{z^{id}} \otimes \mathbb{U}_{z^{exp}}}^T. \quad (2)$$

Thanks to the preserved normal distribution, any pre-trained generative model follows this prior could be used as  $\mathcal{G}$ .

**Neutral Bank.** Since identity-aware sampling guarantees all samples in  $\{X_i\}$  share the same identity, the distribution  $\{q_i^{id}\}$  should be the same according to identity-consistency. Thus, the neutralized 3D face  $\{X_i^n\}$  should roughly be the same. However, enforcing similarity to fulfill identity-consistency alone can be ambiguous regarding the amount of retained identity-relevant information, which leads to a myriad of local minima. As a consequence, the unconstrained  $z^{exp}$  learns to preserve the majority of identity-relevant information, while  $z^{id}$  retains less identity-relevant information. This phenomenon is similar to what was observed in [19] and stated in [34]. This issue could be addressed by maximizing mutual information of  $z^{id}$  and the underlying identity factors.

We consider scans with neutral expression retrain only identity-related information and propose to learn such scans with dedicated inductive biases in the context of weak supervision. Assuming that expression morphing is additive to the neutral face [59], [15], a neutral scan  $s$  from  $n$  scans of same subject  $\{X_i\}$  could be learned through solving an under-determined linear system with least-square constraint:

$$\arg \min_{\sum_i \|\delta_i\|} \begin{bmatrix} s \\ \delta_1 \\ \vdots \\ \delta_n \end{bmatrix} \begin{bmatrix} | & I_{n \times n} \\ | & \end{bmatrix} = \begin{bmatrix} X_1 \\ \vdots \\ X_n \end{bmatrix},$$

where  $s$  is the neutral face,  $\delta_i$  denotes expression-related offsets from  $s$  to the  $i$ -th scan  $X_i$ . These sparse least-square problem could be solved in a closed form as:  $s = \frac{1}{n} \sum_i^n X_i$ ,  $\delta_i = X_i - s$ , where  $\delta_i$  could be effected by both identity and expression. This suggests that an averaging of observed scans can approximately serve as the pseudo neutral scan. In the proposed method, we construct a Neutral Bank module which stores the pseudo neutral scan for each subject and leverages the Exponential Moving Average (EMA) to learn on the fly using the reconstructed faces  $\{X_i^r\}$  belonging to the same subject. Given the selected subject ID,  $K$ , during identity-aware sampling and current step  $t$ , the updating of Neutral Bank module can be formulated as:

$$\mathcal{B}_K^{(t+1)} = \beta \mathcal{B}_K^{(t)} + (1 - \beta) \overline{X}^r, \quad (3)$$

where  $\beta$  is the hyper-parameter of EMA and  $\overline{X}^r$  denotes the average of  $\{X_i^r\}$ . The pseudo neutral scans for subject  $K$ ,  $\mathcal{B}_K$ , are utilized to maximize the identity-relevant information preserved in  $z^{id}$  through the neutralized faces  $\{X_i^n\}$ . Since all samples in  $\{X_i^n\}$  are generated using constant expression code, as in Eq. 1, the subject-specific information could only be encoded by learnable  $z^{id}$ . In this way, with only identity label,  $z^{id}$  learns to preserve identity-related information without ambiguity and achieves identity-consistency implicitly with subject specified  $\mathcal{B}_K$ . It is worth noting that this approach introduces the inductive bias of face deformation (additive) and energy-minimizing (least-square constraint). Compared to using averaged scans as  $\mathcal{B}$ , learning from EMA updated  $\mathcal{B}$  follows a progressive learning principle and Neutral Bank module may benefit from online expression augmentation. Besides, thanks to the agnostic of input topology, the proposed Neutral Bank module could be extended to deal with heterogenous scans.

### B. Loss Functions

The proposed generative framework learns to model 3D faces with disentangled factors in a fashion of VAE. Besides maximizing the Evidence Lower Bound (ELBO) of VAE, auxiliary losses are proposed to disentangle latent spaces through information bottleneck-based mechanism and label-free bijectivity mapping constraint.

**Reconstruction Loss.** With the assumption that all facial scans are registered in the same topology, the likelihood term in ELBO could be defined as reconstruction loss between the input scan  $X$  and the decoded face  $X^r$ :

$$\mathcal{L}_{rec} = \|X - X^r\|^2. \quad (4)$$

**KL Loss.** As for Kullback-Leibler (KL) divergence term in ELBO, we impose KL divergence on two decoupled distributions  $q^{id}$  and  $q^{exp}$  as:

$$\mathcal{L}_{KL} = KL(q^{id} \parallel \mathcal{N}(0, I)) + KL(q^{exp} \parallel \mathcal{N}(0, I)). \quad (5)$$

**Neutralization Loss.** To prevent degeneration of the identity latent space and enforce identity-consistency, the mutual-information between  $z^{id}$  and the underlying identity information is maximized by using the generated neutralized faces  $\{X^n\}$ . We utilize pseudo neutral scans,  $\mathcal{B}_K$ , of  $K$ -th subject from Neutral Bank as a representation of underlying identity information. Similar to  $X^r$ , likelihood is maximized by a reconstruction loss, defined as:

$$\mathcal{L}_{neu} = \alpha_K \|\mathcal{B}_K - X^n\|^2, \quad \alpha_K = 1 - \exp(1 - |K|) \quad (6)$$

where  $|K|$  represents the number of samples for subject  $K$ . The factor  $\alpha_K$  can be interpreted as the confidence score of EMA updated  $\mathcal{B}_K$ , since the EMA updated  $\mathcal{B}_K$  can hardly guarantee to preserve only identity-related information when few variety of expressions of the same subject are demonstrated during training. Identity-consistency across  $\{q_i^{id}\}$  is implicitly learned through reconstruction the same target, which factors expression out of identity space.

TABLE I: Quantitative comparison with other methods on the FaceScape and CoMA datasets.

Dataset	Method	Exp. Label	$E_{avd}$		$E_{id}$		$E_{neu}$	
			mean↓	median↓	mean↓	median↓	mean↓	median↓
FaceScape	FaceTuneGAN	Dense	0.81	0.76	-	-	1.42	1.26
	FED	Sparse	1.370	1.307	0.569	0.551	1.927	1.815
	FED w/o exp. label	-	1.157	1.109	0.765	0.758	3.112	2.957
	<b>Ours</b>	-	<b>1.110</b>	<b>0.998</b>	<b>0.366</b>	<b>0.353</b>	<b>1.590</b>	<b>1.485</b>
CoMA	FaceTuneGAN	Dense	0.83	0.77	0.018	0.018	0.98	0.81
	DRL	Dense	1.413	1.017	0.064	0.062	-	-
	DI-MeshEnc	Dense	0.665	0.434	0.019	0.020	-	-
	IB-VAE	Sparse	0.663	0.643	0.006	0.005	0.051	0.048
	FED	Sparse	0.651	0.625	0.014	0.013	0.065	0.063
	FED w/o exp. label	-	0.783	0.772	0.176	0.180	1.528	1.268
	<b>Ours</b>	-	<b>0.480</b>	<b>0.409</b>	<b>0.005</b>	<b>0.002</b>	<b>0.651</b>	<b>0.697</b>

**Jacobian Loss.** To achieve better disentangled expression representations without label, we enforce the mapping from the *norm* of expression latent code  $z^{exp}$  to the intensity of expression is bijective and leverage energy-minimizing prior. Thus, diverse expressions under the same intensity should be mapped to different directions in  $z^{exp}$ ; otherwise, the decoder is unable to distinguish these expressions. We model the intensity of expression for  $X^r$  as the *norm* of  $X^r - X^n$ . Therefore, this bijective mapping could be described by a non-negative monotonically increasing scalar function  $\sigma$ :  $\sigma' > 0$ , *s.t.*  $(f(y) - f(\vec{0}))^T (f(y) - f(\vec{0})) = \sigma(y^T y)$ , where  $y$  indicates  $z^{exp}$  and  $f(y) = \mathcal{G} \circ \mathcal{R}(z^{id}, y)$ . The subject-specified  $\sigma$  and identity code  $z^{id}$  is omitted for clarity. Since it is hard to explicitly formulate  $\sigma$ , we compute its equivalent form:  $(f(y) - f(\vec{0}))^T J_f(y)y = \sigma'(y^T y)y^T y$ , where  $J_f(y)$  stands for jacobian matrix. This formula suggests that we could further improve disentangled representation learning with energy-minimizing prior by enforcing  $0 \leq (f(y) - f(\vec{0}))^T J_f(y)y \leq \sigma'_{max} y^T y$ . The lower bound enforces a bijectivity mapping which necessitates the incorporation of diverse directions in encoding expressions, while the overall deformation is regularized by the locally defined upper bound. Consequently, the expression space is restricted to exclusively model expression deformation. In this case, instead of finding subject specified  $\sigma'_{max}$ , we constrain it with a hyper parameter  $\gamma > 0$ . We implement such constraint as:

$$\mathcal{L}_{jac} = \max(0, -(X^r - X^n)^T J_{z^{exp}} z^{exp}, (X^r - X^n)^T J_{z^{exp}} z^{exp} - \gamma z^{exp T} z^{exp}), \quad (7)$$

where  $J_{z^{exp}}$  is the jacobian matrix with respect to  $z^{exp}$ , given input  $z^{id}$  and  $z^{exp}$ . Thanks to the MLP generator network  $\mathcal{G}$ , the jacobian matrix could be computed efficiently.

**Identity Compactness Loss.** We also use  $\mathcal{L}_{mi}$  proposed in [43] to enforce compactness of identity branch. Our overall loss function is:

$$\mathcal{L} = \mathcal{L}_{rec} + \mathcal{L}_{KL} + \lambda_{neu} \mathcal{L}_{neu} + \lambda_{jac} \mathcal{L}_{jac} + \lambda_{mi} \mathcal{L}_{mi}. \quad (8)$$

where  $\lambda_{neu}$ ,  $\lambda_{jac}$  and  $\lambda_{mi}$  are hyper-parameters that control and balance different losses.

## IV. EXPERIMENT

### A. Datasets

We evaluate the effectiveness of our approach on publicly available datasets. **CoMA** [39] contains 144 dynamic sequences of 20,466 3D scans from 12 subjects. Following [39], we divide the scans into training and test sets by selecting consecutive 10 frames from every 100 frames as test samples. For evaluation purposes, we consider the facial expression of the first frame of each sequence as *neutral*. Additionally, the average of the frames of the specific subject is served as the *neutral* scan in the test set. **FaceScape** [55] contains static 3D scans of 847 subjects and each subject performs 20 facial expressions (including *neutral*). We follow [19] and select 30% of the subjects randomly as the test set and the rest are used for training. Any scans of the IDs in test set is not demonstrated during training. **D3DFACS** [27], [12] contains 519 dynamic sequences of 46,903 scans from 10 subjects and this dataset is adopted to demonstrate the feasibility of training from combined datasets.

### B. Implementation Details

**Data Preprocessing.** Our method is developed under the assumption that all scans are registered into the same topology, and correspondence learning on heterogeneous scans is beyond the scope of this paper. When training on combined datasets, all heterogeneous scans are registered into the FLAME topology. Rigid pose estimation is performed for better alignment, and we do not consider pose variations. After registration, 5% of training scans with the lowest quality are dropped by performing PCA. The normalization parameters are pre-computed on the remaining training scans.

**Training Setups.** We train the network using AdamW optimizer [32] with common weight decay  $1 \times 10^{-5}$  and batch size of 32, *i.e.*, 8 IDs are selected and 4 scans are drawn from each ID. The network is trained for 100 epochs without data augmentation. Notably,  $\mathcal{L}_{mi}$  is not adopted in FaceScape ( $\lambda_{mi} = 0$ ) due to its relatively strong regularization effect resulting from a large-scale number of identity (847) compared to the latent space dimension (64).

### C. Evaluation Metrics

We adopt Average Vertex Distance (AVD) and the evaluation metrics used in [22], [61], [33], [19] for a fair comparison. The AVD between the reconstructed mesh  $X^r$  and target mesh  $X$  is defined as:  $AVD(X, X^r) = \frac{1}{|V|} \sum_{v=1}^{|V|} \|X(v) - X^r(v)\|_2$ , where  $|V|$  denotes the number of vertices, and  $X(v)$  denotes the  $v$ -th vertex.

**Reconstruction.** The reconstruction error measures information preserved in the generative model, defined as:

$$E_{avd} = AVD(X, X^r). \quad (9)$$

**Disentanglement.** The identity disentanglement metric measures the compactness of the neutralized face  $\{X^n\}$  by standard deviations. This metric is evaluated on all generated neutral meshes  $\{X^n\}$  of the subject as:

$$E_{id} = \text{std}(\|X^n(v) - X^{mean}(v)\|_2), \quad (10)$$

where  $\text{std}()$  denotes standard deviation and  $X^{mean}$  denotes the average over all generated neutral faces  $\{X^n\}$  belonging to currently evaluated subject. A similar disentanglement metric for expression  $E_{exp}$  is defined analogically on all generated samples of the same expression after identity removal.

**Neutralization.** The neutralization error measures the quality of the neutralized face  $X^n$  by calculating the distance between the ground-truth  $X^{neu}$  and the neutralized face, which is defined on each sample as:

$$E_{neu} = AVD(X^{neu}, X^n). \quad (11)$$

### D. Quantitative Comparison

We first compare the proposed WSDF with recent disentanglement methods on the FaceScape and CoMA datasets, including DRL [22], DI-MeshEnc [61], IB-VAE [43], FaceTuneGAN [33] and FED [19]. The quantitative results of reconstruction, disentanglement, and neutralization are shown in Table I. FaceTuneGAN is marked in gray because they employ a different split strategy, using only a portion of scans in CoMA and reserving only 10% of scans for evaluation in FaceScape. On CoMA, the neutralization error  $E_{neu}$  of IBVAE and FED is marked in gray due to test set leakage caused by identical IDs in the training and test sets, coupled with learning neutralization through reconstruction with labeled neutral scans.

When comparing on FaceScape, our method outperforms both FED and FED without expression labels in terms of reconstruction, disentanglement, and neutralization. Notably, our method achieves a 17.4% improvement in neutralization compared to FED, even without the advantage of expression labels. On CoMA, we observe that the compared methods, IBVAE and FED, significantly benefit from information leakage, resulting in superior neutralization performance. Comparing between FED and FED without expression labels on CoMA, we can see that without the aid of expression labels, the neutralization error  $E_{neu}$  of FED increases tremendously ( $23\times$ ). Our method achieves the best reconstruction quality

TABLE II: Results achieved by training on combined datasets.

Dataset	w/ C.D.	$E_{avd}$		$E_{id}$		$E_{exp}$		$E_{neu}$	
		mean $\downarrow$	median $\downarrow$						
FaceScape*	$\times$	0.890	0.806	<b>0.496</b>	<b>0.479</b>	0.516	0.517	1.464	1.375
	$\checkmark$	<b>0.841</b>	<b>0.779</b>	0.513	0.492	<b>0.391</b>	<b>0.392</b>	<b>1.430</b>	<b>1.347</b>
CoMA	$\times$	0.480	0.409	<b>0.005</b>	<b>0.002</b>	-	-	0.651	0.697
	$\checkmark$	<b>0.449</b>	<b>0.401</b>	0.023	0.012	-	-	<b>0.618</b>	<b>0.648</b>

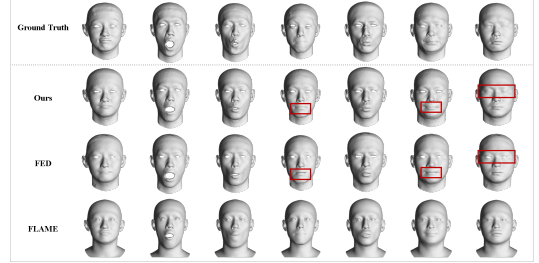


Fig. 2: Qualitative comparison on FaceScape. Zoom in for a better view.

and disentanglement across all approaches and achieves a 47.5% improvement in neutralization compared to its counterpart (FED without expression labels). The comparison clearly validates the effectiveness of the proposed WSDF.

**Training on Combined Datasets.** We assess the generalizability of training our network on combined datasets. The baseline models are individually trained on the CoMA and FaceScape\* datasets (registered in FLAME topology). Subsequently, we train randomly initialized models on combined datasets (with auxiliary training data from D3DFACS) using the same setups.

As shown in Table II, training on combined datasets leads to improvements in reconstruction and neutralization for both datasets. Additionally, it enhances expression disentanglement ( $E_{exp}$ ) due to the increased diversity of expressions, indicating improved generalizability. We attribute the slight reduction in identity disentanglement ( $E_{id}$ ) to the limited representation space (4 dimensions for CoMA, 64 dimensions for FaceScape\*) compared to the expansive corpus of identities covered by the newly introduced D3DFACS dataset. This phenomenon is particularly evident in the CoMA dataset, where the disparity between the data is notably pronounced.

### E. Qualitative Evaluation

**Reconstruction.** We experimentally demonstrate that our model can faithfully reconstruct face scans with unseen IDs. To compare with FED, we directly reconstruct the facial scans in FaceScape test set with the latent codes predicted by the encoders. As illustrated in Fig. 2, compared to the counterparts, our model is more capable of preserving the figure of facial scans and capturing fine structures of mouth and around the eyes.

**Interpolation.** We demonstrate that the learned latent spaces are structured and disentangled by performing interpolation. To be specific, we randomly select pairwise scans in test set (the ID is not observed during training) and

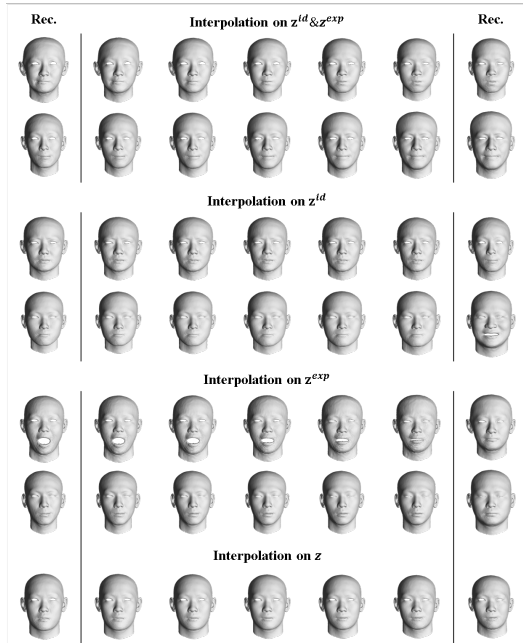


Fig. 3: Interpolation results achieved on FaceScape.

TABLE III: Ablation study on FaceScape.

Designs	$E_{avd}$		$E_{id}$		$E_{exp}$		$E_{neu}$	
	mean↓	median↓	mean↓	median↓	mean↓	median↓	mean↓	median↓
baseline	<b>0.921</b>	<b>0.820</b>	0.994	0.988	1.408	1.400	2.882	2.725
+ neu. bank	1.052	0.955	<b>0.329</b>	<b>0.314</b>	0.956	0.942	1.597	1.498
+ jac. loss	1.110	0.998	0.366	0.353	<b>0.466</b>	<b>0.479</b>	<b>1.590</b>	<b>1.485</b>

calculate their latent codes,  $z^{id}$  and  $z^{exp}$ , by our encoders. Linear interpolations are conducted jointly ( $z^{id}$  &  $z^{exp}$ ) or exclusively (using only  $z^{id}$  or  $z^{exp}$ ). It is important to note that interpolation solely on  $z^{id}$  results in identity-swapping and interpolation solely on  $z^{exp}$  leads to expression transfer. As illustrated in Fig. 3, performing linear interpolations on  $z^{id}$  and  $z^{exp}$  simultaneously generates plausible facial geometries, and interpolation on a single factor (either  $z^{id}$  or  $z^{exp}$ ) generate semantically meaningful variations. This implies that the generation is controlled by decoupled factors that are semantically aligned.

**Neutralization.** We evaluate the disentanglement performance by probing information preserved in  $z^{id}$ . To evaluate this, we select scans with identity and expression changes from the test set (whose IDs and neutralized scans are not seen during training) and calculate their latent codes,  $z^{id}$  and  $z^{exp}$ , using our encoders. We then generate neutralized faces  $X^n$  by Eq. 1 and compare with ground-truth scans. As illustrated in Fig. 4, the generated neutralized faces, using only  $z^{id}$ , faithfully represent identity-specified geometries and remain consistent among different scans of the same individual, suggesting that the majority of identity-relevant information is preserved in  $z^{id}$  without nuisance information.

#### F. Ablation Study

**Effect of Neutral Bank.** We investigate its necessity by training with only  $\mathcal{L}_{rec}$  and  $\mathcal{L}_{KL}$  as the baseline method,

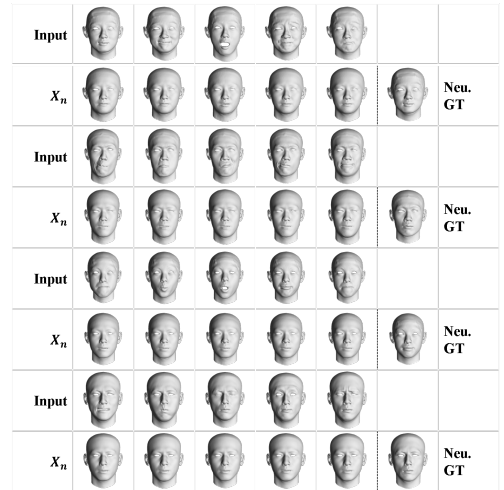


Fig. 4: Neutralization of unseen scans on FaceScape. Each row indicates one individual.

TABLE IV: Ablation study results on CoMA.

Designs	$E_{avd}$		$E_{id}$		$E_{neu}$	
	mean↓	median↓	mean↓	median↓	mean↓	median↓
baseline	<b>0.342</b>	<b>0.305</b>	1.611	1.643	3.147	2.877
+ neu. bank	0.402	0.356	0.017	0.012	0.659	0.704
+ jac. loss	0.447	0.382	0.020	0.014	<b>0.651</b>	<b>0.684</b>
+ mi. loss	0.480	0.409	<b>0.005</b>	<b>0.002</b>	<b>0.651</b>	0.697

no supervision is applied on  $X^n$ . As illustrated in Table III, the baseline method demonstrates proficient reconstruction capabilities, as evidenced by its low  $E_{avd}$ . However, it exhibits shortcomings, as reflected in the elevated values of  $E_{id}$  and  $E_{neu}$ . These higher values suggest that the baseline struggles to disentangle underlying controlling factors, resulting in the inability to generate convincing neutralized faces and maintain consistency in identity representation. Comparatively,  $E_{id}$ ,  $E_{exp}$  and  $E_{neu}$  decrease significantly by adding Neutral Bank (+ neu. bank). This finding supports that the proposed Neutral Bank is crucial for identity-consistency and disentanglement learning. Similarly, this necessity is also evident when training on CoMA as show in Table IV (baseline *v.s.* + neu. bank).

We also qualitatively evaluate Neutral Bank by comparing

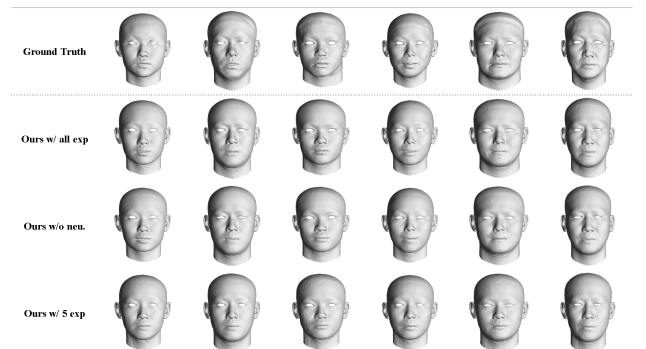


Fig. 5: Visualization of Neutral Bank on FaceScape.

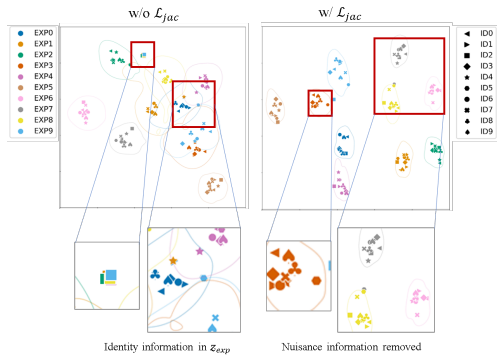


Fig. 6: t-SNE of  $z_{exp}$  on FaceScape test set. Shaped by IDs.

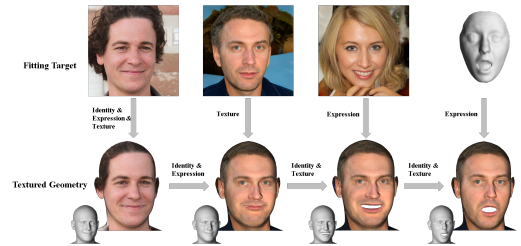
with ground-truth neural scans on FaceScape. As shown in Fig. 5, when training with all expressions (ours w/ all exp), the EMA updated Neutral Bank preserves identity-specified geometries. The model could still capture identity-relevant geometries when neutral scans are excluded from training (ours w/o neu.), and even when only 5 expressions (ours w/ 5 exp) are observed during training. This suggests the robustness of Neutral Bank to the existence of scans with neutral expression and the diversity of expressions.

**Effect of Jacobian Loss.** Incorporating  $\mathcal{L}_{jac}$  to our framework (with a neutralization bank), as presented in Table III, has yielded noteworthy outcomes. Notably, the disentanglement metric  $E_{exp}$  has seen a substantial reduction of 51.2%, indicating a marked improvement. There is a slight decrease in  $E_{neu}$ , and other metrics show marginal impact, attributable to the delicate balance struck among multiple losses. This outcome suggests that the inclusion of the second-order loss,  $\mathcal{L}_{jac}$ , has proven effective in prompting the expression branch to discern and isolate nuisance information, thereby enhancing overall disentanglement. Additionally, on CoMA, the introduction of  $\mathcal{L}_{mi}$  has facilitated a more favorable trade-off between the disentangled factors.

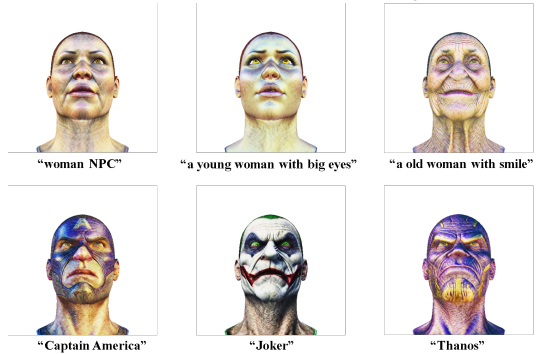
We further performs t-SNE analysis on the predicted  $z_{exp}$  from FaceScape test set. As illustrated in Fig. 6, the expression representations  $z_{exp}$  exhibit identity-based clustering without using  $\mathcal{L}_{jac}$ , indicating the presence of irrelevant information. In contrast, employing  $\mathcal{L}_{jac}$  facilitates eliminating such extraneous information, where the clustering of  $z_{exp}$  is only associated with expression categories.

### G. Application

The learned generative 3D face model achieves controllability via disentanglement learning and it can be applied to a number of downstream tasks. In Fig. 7(a), we provide 3D face reconstruction (first column), texture transfer (second column) and expression transfer (third column) results by fitting 2D images (generated by StyleGAN2 [24]), and the expression transfer result (last column) by fitting 3D scan (from BU-3DFE [58]). Texture transfer and expression transfer are achieved by swapping the fitted texture maps and expression latent codes. Similarly to 2D expression transfer, the expression is transferred by exchanging expression latent codes.



(a) Reconstruction and editing.



(b) Text-to-3D generation.

Fig. 7: Examples of downstream applications.

Fig. 7(b) provides text-to-3D generation by utilizing our decoding components, the pre-trained diffusion model [40] and SDS loss [37]. Our pipeline draws inspiration from Fantasia3D [9] and utilizes a mesh-based differentiable renderer [26] to simultaneously optimize parameterized geometry and texture. Thanks to our mesh-based 3D representation, the generation pipeline is efficient and it takes only 15 minutes to optimize a 3D face on a single RTX 3090.

## V. CONCLUSIONS

This paper presents a method for controllable 3D face modeling with weakly-supervised training. The Neutral Bank module utilizes identity labels to learn pseudo ground-truth, enforcing identity-consistency along with information preservation through an auxiliary loss function. Additionally, a label-free second-order loss function is designed to further enhance disentanglement by imposing regularization on the latent expression space. Experimental results demonstrate that the proposed WSDF is effective in learning a controllable 3D face model. This study also validates the potential of learning 3D face models from multiple collections.

## VI. ACKNOWLEDGMENTS

This work is partly supported by the National Key R&D Program of China (No. 2022ZD0161902), the National Natural Science Foundation of China (No. 62176012, 62202031), and the Beijing Natural Science Foundation (No. 4222049).

## REFERENCES

- [1] B. Amberg, R. Knothe, and T. Vetter. Expression invariant 3d face recognition with a morphable model. In *2008 8th IEEE International Conference on Automatic Face & Gesture Recognition*, pages 1–6, 2008.

- [2] T. Bagautdinov, C. Wu, J. Saragih, P. Fua, and Y. Sheikh. Modeling facial geometry using compositional vaes. In *2018 IEEE/CVF Conference on Computer Vision and Pattern Recognition*, pages 3877–3886, 2018.
- [3] M. Bahri, E. O’ Sullivan, S. Gong, F. Liu, X. Liu, M. M. Bronstein, and S. Zafeiriou. Shape my face: Registering 3d face scans by surface-to-surface translation. *International Journal of Computer Vision*, 129(9):2680–2713, Sep 2021.
- [4] V. Blanz and T. Vetter. A morphable model for the synthesis of 3d faces. In *Proceedings of the 26th Annual Conference on Computer Graphics and Interactive Techniques, SIGGRAPH ’99*, page 187–194, USA, 1999. ACM Press/Addison-Wesley Publishing Co.
- [5] V. Blanz and T. Vetter. Face recognition based on fitting a 3d morphable model. *IEEE Transactions on Pattern Analysis and Machine Intelligence*, 25(9):1063–1074, 2003.
- [6] J. Booth, A. Roussos, S. Zafeiriou, A. Ponniah, and D. Dunaway. A 3d morphable model learnt from 10,000 faces. In *2016 IEEE Conference on Computer Vision and Pattern Recognition (CVPR)*, pages 5543–5552, 2016.
- [7] G. Bouritsas, S. Bokhnyak, S. Ploumpis, S. Zafeiriou, and M. Bronstein. Neural 3d morphable models: Spiral convolutional networks for 3d shape representation learning and generation. In *2019 IEEE/CVF International Conference on Computer Vision (ICCV)*, pages 7212–7221, 2019.
- [8] C. Cao, Y. Weng, S. Zhou, Y. Tong, and K. Zhou. Facewarehouse: A 3d facial expression database for visual computing. *IEEE Transactions on Visualization and Computer Graphics*, 20(3):413–425, 2014.
- [9] R. Chen, Y. Chen, N. Jiao, and K. Jia. Fantasia3d: Disentangling geometry and appearance for high-quality text-to-3d content creation. In *Proceedings of the IEEE/CVF International Conference on Computer Vision (ICCV)*, October 2023.
- [10] R. T. Q. Chen, X. Li, R. B. Grosse, and D. K. Duvenaud. Isolating sources of disentanglement in variational autoencoders. In S. Bengio, H. Wallach, H. Larochelle, K. Grauman, N. Cesa-Bianchi, and R. Garnett, editors, *Advances in Neural Information Processing Systems*, volume 31. Curran Associates, Inc., 2018.
- [11] D. Clevert, T. Unterthiner, and S. Hochreiter. Fast and accurate deep network learning by exponential linear units (elus). In Y. Bengio and Y. LeCun, editors, *4th International Conference on Learning Representations, ICLR 2016, San Juan, Puerto Rico, May 2-4, 2016, Conference Track Proceedings*, 2016.
- [12] D. Cosker, E. Krumhuber, and A. Hilton. A face valid 3d dynamic action unit database with applications to 3d dynamic morphable facial modeling. In *2011 International Conference on Computer Vision*, pages 2296–2303, 2011.
- [13] R. Danecek, M. J. Black, and T. Bolkart. EMOCA: Emotion driven monocular face capture and animation. In *Conference on Computer Vision and Pattern Recognition (CVPR)*, pages 20311–20322, 2022.
- [14] Y. Deng, J. Yang, S. Xu, D. Chen, Y. Jia, and X. Tong. Accurate 3d face reconstruction with weakly-supervised learning: From single image to image set. In *2019 IEEE/CVF Conference on Computer Vision and Pattern Recognition Workshops (CVPRW)*, pages 285–295, 2019.
- [15] B. Egger, W. A. P. Smith, A. Tewari, S. Wuhler, M. Zollhoefer, T. Beeler, F. Bernard, T. Bolkart, A. Kortylewski, S. Romdhani, C. Theobalt, V. Blanz, and T. Vetter. 3d morphable face models—past, present, and future. *ACM Trans. Graph.*, 39(5), jun 2020.
- [16] S. Galanakis, B. Gecer, A. Lattas, and S. Zafeiriou. 3dmm-rf: Convolutional radiance fields for 3d face modeling. In *Proceedings of the IEEE/CVF Winter Conference on Applications of Computer Vision (WACV)*, pages 3536–3547, January 2023.
- [17] T. Gerig, A. Morel-Forster, C. Blumer, B. Egger, M. Luthi, S. Schoenborn, and T. Vetter. Morphable face models - an open framework. In *2018 13th IEEE International Conference on Automatic Face & Gesture Recognition (FG 2018)*, pages 75–82, 2018.
- [18] S. Gong, L. Chen, M. Bronstein, and S. Zafeiriou. Spiralnet++: A fast and highly efficient mesh convolution operator. In *2019 IEEE/CVF International Conference on Computer Vision Workshop (ICCVW)*, pages 4141–4148, 2019.
- [19] Y. Gu, N. Pears, and H. Sun. Adversarial 3d face disentanglement of identity and expression. In *2023 IEEE 17th International Conference on Automatic Face and Gesture Recognition (FG)*, pages 1–7, 2023.
- [20] I. Higgins, L. Matthey, A. Pal, C. P. Burgess, X. Glorot, M. M. Botvinick, S. Mohamed, and A. Lerchner. beta-vae: Learning basic visual concepts with a constrained variational framework. In *5th International Conference on Learning Representations, ICLR 2017, Toulon, France, April 24-26, 2017, Conference Track Proceedings*. OpenReview.net, 2017.
- [21] Y. Hong, B. Peng, H. Xiao, L. Liu, and J. Zhang. Headerf: A real-time nerf-based parametric head model. In *IEEE/CVF Conference on Computer Vision and Pattern Recognition (CVPR)*, 2022.
- [22] Z.-H. Jiang, Q. Wu, K. Chen, and J. Zhang. Disentangled representation learning for 3d face shape. In *2019 IEEE/CVF Conference on Computer Vision and Pattern Recognition (CVPR)*, pages 11949–11958, 2019.
- [23] A. Kacem, K. Cherenkova, and D. Aouada. Disentangled face identity representations for joint 3d face recognition and neutralisation. In *2022 8th International Conference on Virtual Reality (ICVR)*, pages 438–443, 2022.
- [24] T. Karras, M. Aittala, J. Hellsten, S. Laine, J. Lehtinen, and T. Aila. Training generative adversarial networks with limited data. In *Proc. NeurIPS*, 2020.
- [25] G. Kwon and J. C. Ye. Diagonal attention and style-based gan for content-style disentanglement in image generation and translation. In *Proceedings of the IEEE/CVF International Conference on Computer Vision*, pages 13980–13989, 2021.
- [26] S. Laine, J. Hellsten, T. Karras, Y. Seol, J. Lehtinen, and T. Aila. Modular primitives for high-performance differentiable rendering. *ACM Transactions on Graphics*, 39(6), 2020.
- [27] T. Li, T. Bolkart, M. J. Black, H. Li, and J. Romero. Learning a model of facial shape and expression from 4d scans. *ACM Trans. Graph.*, 36(6), nov 2017.
- [28] J. Ling, Z. Wang, M. Lu, Q. Wang, C. Qian, and F. Xu. Semantically disentangled variational autoencoder for modeling 3d facial details. *IEEE Transactions on Visualization and Computer Graphics*, pages 1–1, 2022.
- [29] F. Liu, L. Tran, and X. Liu. 3d face modeling from diverse raw scan data. In *2019 IEEE/CVF International Conference on Computer Vision (ICCV)*, pages 9407–9417, 2019.
- [30] F. Liu, Q. Zhao, X. Liu, and D. Zeng. Joint face alignment and 3d face reconstruction with application to face recognition. *IEEE Transactions on Pattern Analysis and Machine Intelligence*, 42(3):664–678, 2020.
- [31] F. Locatello, S. Bauer, M. Lucic, G. Raetsch, S. Gelly, B. Schölkopf, and O. Bachem. Challenging common assumptions in the unsupervised learning of disentangled representations. In *International Conference on Machine Learning*, pages 4114–4124, 2019.
- [32] I. Loshchilov and F. Hutter. Fixing weight decay regularization in adam. *CoRR*, abs/1711.05101, 2017.
- [33] N. Olivier, K. Baert, F. Danieau, F. Multon, and Q. Avril. Facetunegan: Face autoencoder for convolutional expression transfer using neural generative adversarial networks. *Comput. Graph.*, 110(C):69–85, mar 2023.
- [34] Y. Pang, Y. Zhang, W. Quan, Y. Fan, X. Cun, Y. Shan, and D.-m. Yan. Dpe: Disentanglement of pose and expression for general video portrait editing. *arXiv preprint arXiv:2301.06281*, 2023.
- [35] P. Paysan, R. Knothe, B. Amberg, S. Romdhani, and T. Vetter. A 3d face model for pose and illumination invariant face recognition. In *2009 Sixth IEEE International Conference on Advanced Video and Signal Based Surveillance*, pages 296–301, 2009.
- [36] S. Ploumpis, H. Wang, N. Pears, W. A. P. Smith, and S. Zafeiriou. Combining 3d morphable models: A large scale face-and-head model. In *2019 IEEE/CVF Conference on Computer Vision and Pattern Recognition (CVPR)*, pages 10926–10935, 2019.
- [37] B. Poole, A. Jain, J. T. Barron, and B. Mildenhall. Dreamfusion: Text-to-3d using 2d diffusion. In *The Eleventh International Conference on Learning Representations, ICLR 2023, Kigali, Rwanda, May 1-5, 2023*. OpenReview.net, 2023.
- [38] M. B. R. A. Tewari, H.-P. Seidel, M. Elgharib, and C. Theobalt. Learning complete 3d morphable face models from images and videos. In *2021 IEEE/CVF Conference on Computer Vision and Pattern Recognition (CVPR)*, pages 3360–3370, 2021.
- [39] A. Ranjan, T. Bolkart, S. Sanyal, and M. J. Black. Generating 3D faces using convolutional mesh autoencoders. In *European Conference on Computer Vision (ECCV)*, pages 725–741, 2018.
- [40] R. Rombach, A. Blattmann, D. Lorenz, P. Esser, and B. Ommer. High-resolution image synthesis with latent diffusion models. In *Proceedings of the IEEE/CVF Conference on Computer Vision and Pattern Recognition (CVPR)*, pages 10684–10695, June 2022.
- [41] R. Shu, Y. Chen, A. Kumar, S. Ermon, and B. Poole. Weakly supervised disentanglement with guarantees. In *8th International Conference on Learning Representations, ICLR 2020, Addis Ababa, Ethiopia, April 26-30, 2020*. OpenReview.net, 2020.
- [42] W. A. P. Smith, A. Seck, H. Dee, B. Tiddeman, J. B. Tenenbaum, and B. Egger. A morphable face albedo model. In *2020 IEEE/CVF Conference on Computer Vision and Pattern Recognition (CVPR)*,

pages 5010–5019, 2020.

- [43] H. Sun, N. Pears, and Y. Gu. Information bottlenecked variational autoencoder for disentangled 3d facial expression modelling. In *2022 IEEE/CVF Winter Conference on Applications of Computer Vision (WACV)*, pages 2334–2343, 2022.
- [44] J. Sun, X. Wang, L. Wang, X. Li, Y. Zhang, H. Zhang, and Y. Liu. Next3d: Generative neural texture rasterization for 3d-aware head avatars. In *CVPR*, 2023.
- [45] A. Tewari, F. Bernard, P. Garrido, G. Bharaj, M. Elgharib, H.-P. Seidel, P. Pérez, M. Zollhöfer, and C. Theobalt. Fml: Face model learning from videos. In *2019 IEEE/CVF Conference on Computer Vision and Pattern Recognition (CVPR)*, pages 10804–10814, 2019.
- [46] J. Thies, M. Zollhöfer, M. Stamminger, C. Theobalt, and M. Nießner. Face2face: Real-time face capture and reenactment of rgb videos. *Commun. ACM*, 62(1):96–104, dec 2018.
- [47] L. Tran, F. Liu, and X. Liu. Towards high-fidelity nonlinear 3d face morphable model. In *In Proceeding of IEEE Computer Vision and Pattern Recognition*, Long Beach, CA, June 2019.
- [48] L. Tran and X. Liu. Nonlinear 3d face morphable model. In *IEEE Computer Vision and Pattern Recognition (CVPR)*, Salt Lake City, UT, June 2018.
- [49] L. Tran and X. Liu. On learning 3d face morphable model from in-the-wild images. *IEEE Trans. Pattern Anal. Mach. Intell.*, 43(1):157–171, jan 2021.
- [50] D. Ulyanov, A. Vedaldi, and V. Lempitsky. Instance normalization: The missing ingredient for fast stylization, 2017.
- [51] D. Vlasic, M. Brand, H. Pfister, and J. Popović. Face transfer with multilinear models. *ACM Trans. Graph.*, 24(3):426–433, jul 2005.
- [52] D. Vlasic, M. Brand, H. Pfister, and J. Popovic. Face transfer with multilinear models. In *ACM SIGGRAPH 2006 Courses*, SIGGRAPH '06, page 24–es, New York, NY, USA, 2006. Association for Computing Machinery.
- [53] L. Wang, Z. Chen, T. Yu, C. Ma, L. Li, and Y. Liu. Faceverse: a fine-grained and detail-controllable 3d face morphable model from a hybrid dataset. In *IEEE Conference on Computer Vision and Pattern Recognition (CVPR2022)*, June 2022.
- [54] Y. Wu, Y. Deng, J. Yang, F. Wei, C. Qifeng, and X. Tong. Anifacegan: Animatable 3d-aware face image generation for video avatars. In *Advances in Neural Information Processing Systems*, 2022.
- [55] H. Yang, H. Zhu, Y. Wang, M. Huang, Q. Shen, R. Yang, and X. Cao. Facescape: a large-scale high quality 3d face dataset and detailed riggable 3d face prediction. In *Proceedings of the IEEE Conference on Computer Vision and Pattern Recognition (CVPR)*, 2020.
- [56] X. Yang and T. Taketomi. Bareskinnet: De-makeup and de-lighting via 3d face reconstruction. *Computer Graphics Forum*, 41(7):623–634, 2022.
- [57] T. Yenamandra, A. Tewari, F. Bernard, H.-P. Seidel, M. Elgharib, D. Cremers, and C. Theobalt. i3dmm: Deep implicit 3d morphable model of human heads. In *2021 IEEE/CVF Conference on Computer Vision and Pattern Recognition (CVPR)*, pages 12798–12808, 2021.
- [58] L. Yin, X. Wei, Y. Sun, J. Wang, and M. Rosato. A 3d facial expression database for facial behavior research. In *7th International Conference on Automatic Face and Gesture Recognition (FG06)*, pages 211–216, 2006.
- [59] W. Zhang, X. Ji, K. Chen, Y. Ding, and C. Fan. Learning a facial expression embedding disentangled from identity. In *2021 IEEE/CVF Conference on Computer Vision and Pattern Recognition (CVPR)*, pages 6755–6764, 2021.
- [60] Z. Zhang, R. Chen, W. Cao, Y. Tai, and C. Wang. Learning neural proto-face field for disentangled 3d face modeling in the wild. In *Proceedings of the IEEE/CVF Conference on Computer Vision and Pattern Recognition (CVPR)*, pages 382–393, June 2023.
- [61] Z. Zhang, C. Yu, H. Li, J. Sun, and F. Liu. Learning distribution independent latent representation for 3d face disentanglement. In *2020 International Conference on 3D Vision (3DV)*, pages 848–857, 2020.
- [62] M. Zheng, H. Yang, D. Huang, and L. Chen. Imface: A nonlinear 3d morphable face model with implicit neural representations. In *Proceedings of the IEEE/CVF Conference on Computer Vision and Pattern Recognition*, pages 20343–20352, 2022.